Supporting Information

Distribution of high valence Fe active sites in nickel-iron hydroxide catalysts for water oxidation

Peijia Ding[a], Qi Hu*[a,b], Ziwei Chai[c], Hong-Bo Zhou[a], Guang-Hong Lu[a], Gilberto Teobaldi[d], Annabella Selloni*[e] and Li-Min Liu*[a]

[a] School of Physics, Beihang University, Beijing 100191, China

[b] School of Chemistry, Beihang University, Beijing 100191, China

[c] Department of Chemistry, University of Zurich, Zurich, Switzerland

[d] Scientific Computing Department, STFC UKRI, Rutherford Appleton Laboratory, Harwell Campus, OX11 0QX Didcot, United Kingdom

[e] Department of Chemistry, Princeton University, Princeton, NJ 08544, USA

Email: liminliu@buaa.edu.cn; huqi@buaa.edu.cn; aselloni@princeton.edu

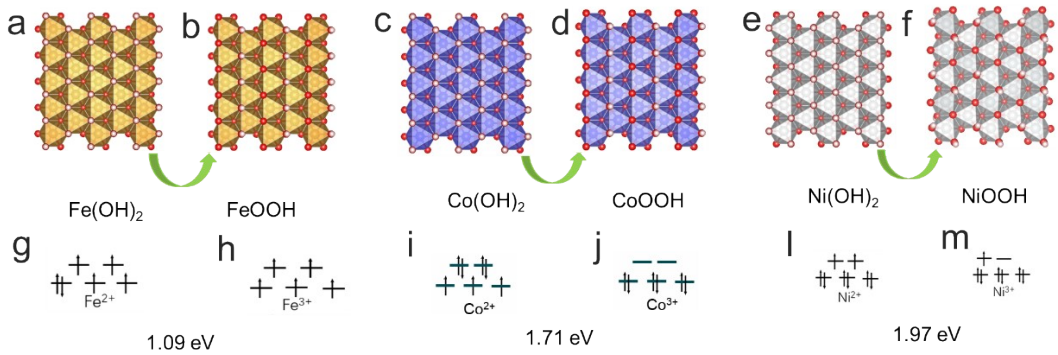

Fig. S1. Structures of $M(OH)_2$ and MOOH (M=Fe, Co, Ni). (**a-f**). Top views of $Fe(OH)_2$, FeOOH, $Co(OH)_2$, CoOOH, $Ni(OH)_2$ and NiOOH, respectively. (**g-m**) Electronic d orbital occupancies of metal ions in (**a-f**).

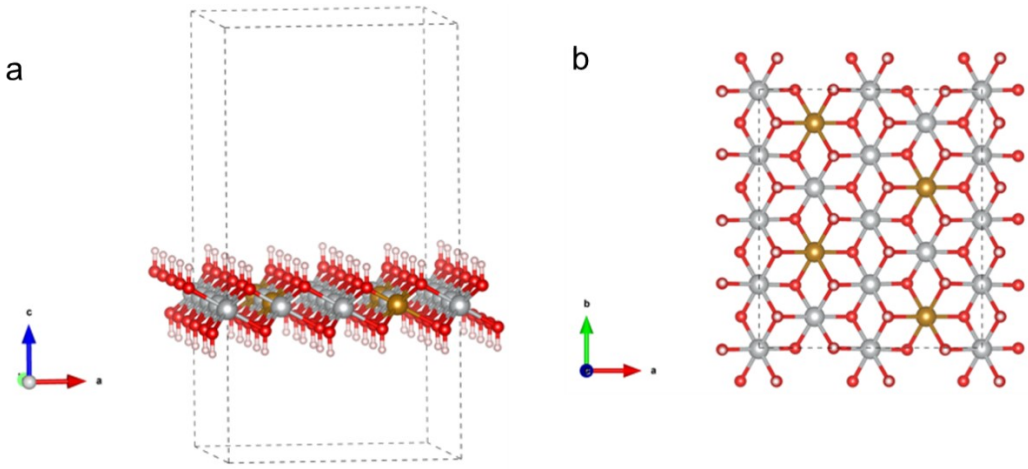

Fig. S2. Single-layer 25% Fe doped NiFe hydroxide, $Ni_{3/4}Fe_{1/4}(OH)_2$, model used for the calculations: (**a**) viewed from the side; (**b**) viewed from above the surface. Grey, red, pinky white and brown balls represent Ni, O, H and Fe atoms, respectively.

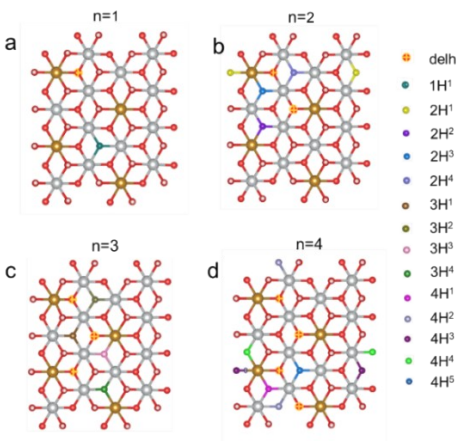

Fig. S3. (**a-d**) The investigated hydrogen desorption sites for $Ni_{3/4}Fe_{1/4}(OH)_2$ in the first stage of the dehydrogenation process (n=1-4). The different colors indicate different nH^x (n=1-4; x=1-5) dehydrogenation sites, as shown by the small balls on the right. Here, n represents the number of desorbed H, and x labels different desorption sites for the same n. The grey, pinky white, brown and red balls represent the Ni, H, Fe and O atoms, respectively.

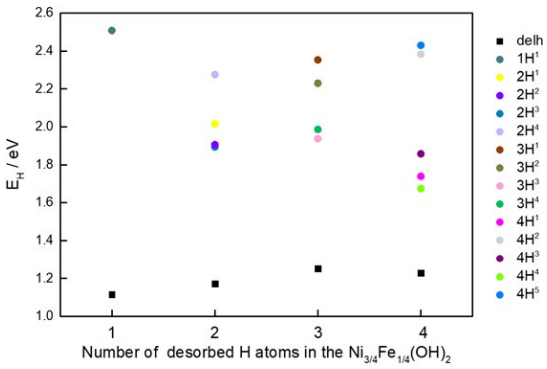

Fig. S4. Desorption energies E_H of different sites in $Ni_{3/4}Fe_{1/4}(OH)_2$ during the dehydrogenation (n=1-4). Black symbols represent the best site. The colors indicate the different dehydrogenation sites shown in **Fig. S3**.

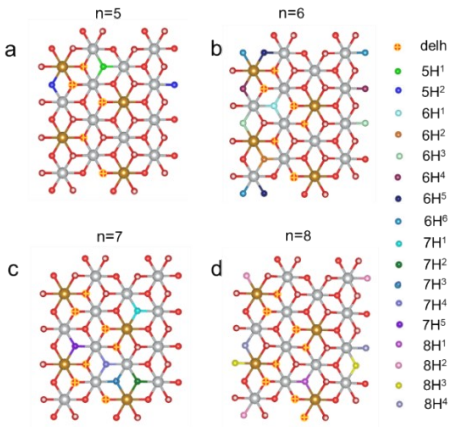

Fig. S5. (**a-d**) The investigated hydrogen desorption sites of $Ni_{3/4}Fe_{1/4}(OH)_2$ during the dehydrogenation process (n=5-8). The different colors indicate different dehydrogenation sites.

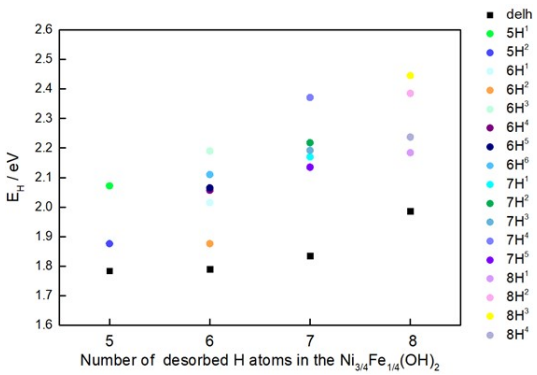

Fig. S6. Desorption energies E_H of different sites in $Ni_{3/4}Fe_{1/4}(OH)_2$ during the second stage of dehydrogenation (n=5-8). Black symbols represent the most favorable site. The different colors correspond to the different dehydrogenation sites shown in **Fig. S5**.

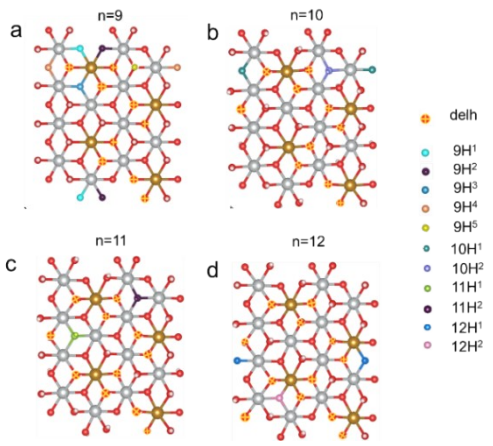

Fig. S7. (**a-d**) The investigated hydrogen desorption sites of $Ni_{3/4}Fe_{1/4}(OH)_2$ during the dehydrogenation process (n=9-12). The different colors indicate different dehydrogenation sites.

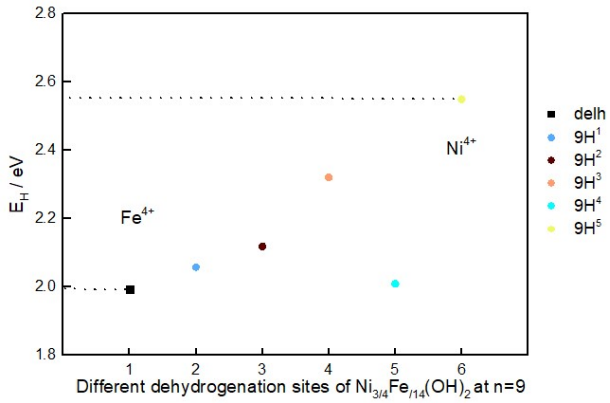

Fig. S8. Desorption energies E_H of different sites in $Ni_{3/4}Fe_{1/4}(OH)_2$ (n=9). Black symbols represent the most favorable site. The different colors indicate the different dehydrogenation sites as shown in **Fig. S7**. $Fe^{4+}$and Ni^{4+} represent the electronic state of black label and olivine label respectively.

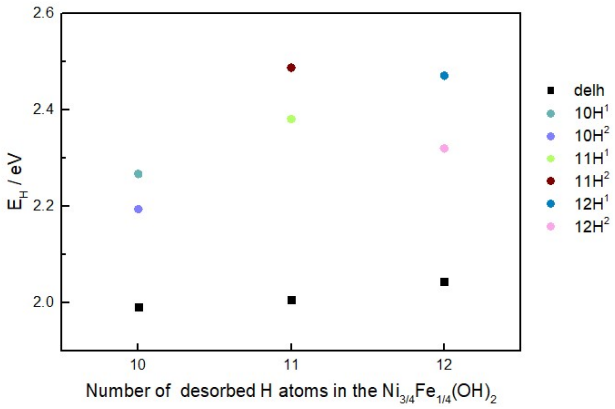

pin

Fig. S9. Desorption energies E_H of different sites in $Ni_{3/4}Fe_{1/4}(OH)_2$ (n=10-12). Black symbols represent the most favorable site. The different colors indicate the different dehydrogenation sites as shown in **Fig. S7**. $Fe^{4+}$and Ni^{4+} represent the electronic state of black label and purple label respectively.

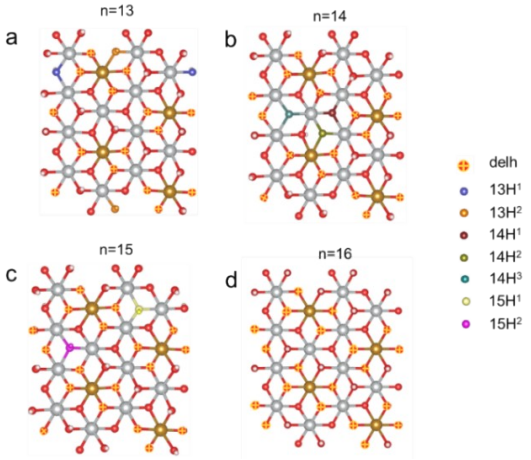

Fig. S10. (a-d) The investigated hydrogen desorption sites of $Ni_{3/4}Fe_{1/4}(OH)_2$ during the dehydrogenation process (n=13-16). The different colors indicate different dehydrogenation sites.

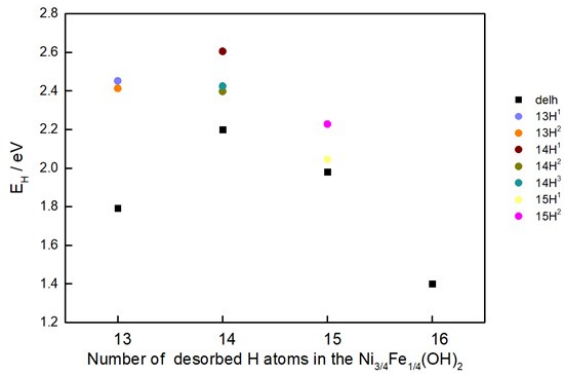

Fig. S11. Desorption energies E_H of different sites in $Ni_{3/4}Fe_{1/4}(OH)_2$ (n=13-16). Black symbols represent the most favorable site. The different colors indicate the different dehydrogenation sites as shown in **Fig. S10**. $Fe^{4+}$and Ni^{4+} represent the electronic state of black label and purple label respectively.

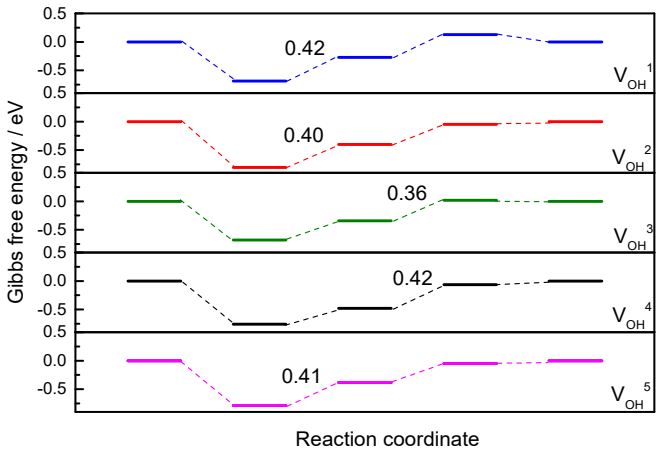

Fig. S12. Calculated OER free energy profiles for the V_{OH}^1, V_{OH}^2, V_{OH}^1, V_{OH}^4 and V_{OH}^5 sites in $Ni_{12}Fe_4O_{32}H_{18}$ (n=14) that are at the top of the volcano plot in **Fig. 4a** of the main text. The reported value in each plot indicates the corresponding OER overpotential (in eV).

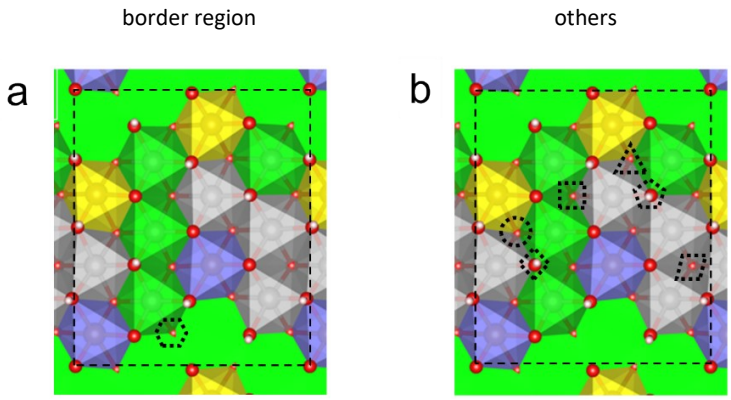

Fig. S13. Locations of the investigated V_{OH} reactive sites in $Ni_{12}Fe_4O_{32}H_{18}$ (n=14), in addition to those shown in **Fig. 4b**: (**a**) site at the border of the Ni^{3+} region between Fe^{3+} and Fe^{4+}; (**b**) sites in non-border region. Green, yellow, purple and grey polyhedral represent Ni^{3+}, Fe^{3+}, Fe^{4+} and Ni^{2+}, respectively. Green area: Ni^{3+} region between Fe^{3+} and Fe^{4+}.

Table S1. Average dehydrogenation energy E_H for the transformation of $M(OH)_2$ to MOOH (M=Fe, Co, Ni), obtained from PBE+U calculations.

Struct.	Total energy / eV	$\triangle E_H$ / eV
Fe $(OH)_2$	-458.18	
FeOOH	-387.02	1.09
$Co(OH)_2$	-428.08	
CoOOH	-347.17	1.71
Ni $(OH)_2$	-395.77	
NiOOH	-310.73	1.96

Table S2. Computed (PBE+U) energies of $Ni_{3/4}Fe_{1/4}OOH$ configurations with different H distributions.

Hydrogen Distribution in $Ni_{3/4}Fe_{1/4}OOH$	Energy / eV	△E / eV
Same as in NiOOH-U[11]	-329.25	0.00
From step-by-step dehydrogenation of $Ni_{3/4}Fe_{1/4}(OH)_2$	-329.59	-0.34

Table S3. Calculated (PBE+U) total energy E, zero-point energy (ZPE) and room temperature. entropy correction (TS) for gas phase H_2 and H_2O. All values are in eV.

	E	ZPE	TS	G / eV
H_2	-6.77	0.28	0.41	-6.90
H_2O	-14.23	0.58	0.67	-14.32

Table S4. Computed (PBE+U) energies of $Ni_{3/4}Fe_{1/4}OH$ configurations at n=12 with different H distributions.

Structure	Total energy / eV	△E / eV
Used in the text	-350.365	0.00
$9H^1$-type (Ni^{3+})	-350.185	0.18

Table S5. Calculated (PBE+U) free energies of the four OER intermediates for the seven different V_{OH} reactive sites in $Ni_{12}Fe_4O_{32}H_{18}$ (n=14) that are shown in **Fig. S12**.

Defect Types	Reaction Step (Formula)	Reactive Site	G-n*1.23/e / V	Overpotential / V	□
	* + $2H_2O$		0.00		
	*OH + H_2O + 1/$2H_2$		-0.71		
	*O + H_2O + H_2		0.00	0.72	
	*OOH + 3/$2H_2$		0.10		
□	* + O_2 + $2H_2$		0.00	□	
	* + $2H_2O$		0.00		
	*OH + H_2O + 1/$2H_2$		-0.92		
others	*O + H_2O + H_2		-0.43	0.48	
	*OOH + 3/$2H_2$		-0.24		
□	* + O_2 + $2H_2$	□	0.00		□
	* + $2H_2O$		0.00		
	*OH + H_2O + 1/$2H_2$		-0.72		
	*O + H_2O + H_2		-0.23	0.49	
	*OOH + 3/$2H_2$		0.16		
□	* + O_2 + $2H_2$	□	0.00		□
	* + $2H_2O$		0.00		
	*OH + H_2O + 1/$2H_2$		-1.01		
border region	*O + H_2O + H_2		-0.77		
	*OOH + 3/$2H_2$		-0.25	0.51	
□	* + O_2 + $2H_2$	□	0.00		□
	* + $2H_2O$		0.00		
	*OH + H_2O + 1/$2H_2$		-0.79		
	*O + H_2O + H_2		-0.38	0.41	
	*OOH + 3/$2H_2$		-0.05		
□	* + O_2 + $2H_2$	□	0.00		□
	* + $2H_2O$		0.00		
	*OH + H_2O + 1/$2H_2$		-0.63		
others	*O + H_2O + H_2		-0.05	0.58	
	*OOH + 3/$2H_2$		0.20		
□	* + O_2 + $2H_2$	□	0.00		□
	* + $2H_2O$		0.00		
	*OH + H_2O + 1/$2H_2$		-0.87		
	*O + H_2O + H_2		-0.58		
	*OOH + 3/$2H_2$		0.00	0.58	
□	* + O_2 + $2H_2$	□	0.00		□